Green Chemistry

Depolymerization of lignin for biological conversion through sulfonation and a chelator-mediated Fenton reaction

Journal:	*Green Chemistry*
Manuscript ID	GC-ART-10-2021-003854.R1
Article Type:	Paper
Date Submitted by the Author:	14-Dec-2021

Complete List of Authors:	Martinez, Daniella; Sandia National Laboratories Rodriguez, Alberto; Joint BioEnergy Institute, Deconstruction; Sandia National Laboratories, Juarros, Miranda; Sandia National Laboratories Martinez, Estevan; Sandia National Laboratories Alam, Todd; Sandia National Laboratory, Electronic and Nanostructured Materials Simmons, Blake; E O Lawrence Berkeley National Laboratory, Biological Systems and Engineering Sale, Kenneth; Joint BioEnergy Institute, Enzyme Optimization Group; Sandia National Laboratories, Biomass Science and Conversion Technology Singer, Steven; Lawrence Berkeley National Laboratory, Kent, Michael; Joint BioEnergy Institute; Sandia National Laboratories,

Green Chemistry

PAPER

Depolymerization of lignin for biological conversion through sulfonation and a chelator-mediated Fenton reaction

Daniella V. Martinez[§1], Alberto Rodriguez[†,§1], Miranda A. Juarros[§], Estevan J. Martinez[§], Todd M. Alam,[§] Blake A. Simmons[†,], Kenneth L. Sale[†,§], Steven W. Singer[†,*], Michael S. Kent[†,§,**]*

Generating value from lignin through depolymerization and biological conversion to valuable fuels, chemicals, or intermediates has great promise but is limited by several factors including lack of cost-effective depolymerization methods, toxicity within the breakdown products, and low bioconversion of the breakdown products. High yield depolymerization of natural lignins requires cleaving carbon-carbon bonds in addition to ether bonds. To address that need, we report that a chelator-mediated Fenton reaction can efficiently cleave C-C bonds in sulfonated polymers at or near room temperature, and that unwanted repolymerization can be minimized through optimizing reaction conditions. This method was used to depolymerize lignosulfonate from M_w = 28,000 g/mol to M_w = 800 g/mol. The breakdown products were characterized by SEC, FTIR and NMR and evaluated for bioavailability. The breakdown products are rich in acid, aldehyde, and alcohol functionalities but are largely devoid of aromatics and aliphatic dienes. A panel of nine organisms were tested for the ability to grow on the breakdown products. Growth at a low level was observed for several monocultures on the depolymerized LS in absence of glucose. Much stronger growth was observed in the presence of 0.2% glucose and for one organism we demonstrate doubling of melanin production in the presence of depolymerized LS. The results suggest that this chelator-mediated Fenton method is a promising new approach for biological conversion of lignin into higher value chemicals or intermediates.

Received 00th January 20xx,
Accepted 00th January 20xx

DOI: 10.1039/x0xx00000x

www.rsc.org/

1. Introduction

Lignin constitutes about 15-30% of the dry weight of plant biomass and is comprised mostly of three monolignols that are polymerized through a variety of interunit C-C and C-O linkages in an irregular fashion. Lignin provides structural integrity to the plant cell walls, and consequently is highly resistant to deconstruction. Yet removing, altering, or depolymerizing lignin is critical to the establishment of lignocellulosic biomass-based industries. Furthermore, generating value from lignin has the potential to contribute significantly to the overall economic viability of a lignocellulosic biorefinery [1-3].

Due to the structural and chemical complexity of lignin, depolymerization inevitably leads to a distribution of breakdown products. Separating components of the complex mixture for upgrading is difficult and expensive. Biological conversion is a promising approach to deal with the complexity of the lignin breakdown products [4-9]. Yet this approach has its own challenges, such as integrating depolymerization processes with fermentation, toxicity of some of the breakdown products, a limited molecular weight range for rapid internalization by bacteria or fungi, and engineering pathways in microbes to funnel the carbon to useful products or intermediates in high yield.

Prior work on depolymerizing lignin has focused on cleaving ether bonds to release aromatic monomers [10-16]. However, whereas most interunit linkages in native lignin are ether bonds, carbon-carbon bonds make up a significant fraction of native lignin linkages and may be increased during some extraction processes. For lignins with 50% β-O-4 content, in theory only about 50% of the lignin can be released as monomers and dimers through cleaving ether bonds and in practice the yield is typically in the range of 20% or less [14, 17, 18]. Higher monomer yields have been achieved for lignins containing higher β-O-4 content (50-70%) through lignin-first processing of intact biomass thereby avoiding isolation processes that result in condensation [13, 19-22] or by altering the natural lignin synthetic pathways [11]. Catalytic approaches performed at high temperature and high pressure may cleave C-C bonds along with C-O bonds resulting in increased monomer yields [22-25]. The monomer yield is often limited by repolymerization of the breakdown products, although this problem has been reduced through the use of protecting groups [11, 26] or careful control of catalyst and conditions [22]. However, the higher monomer yields with lignin-first approaches and catalytic depolymerization approaches at high temperature and high pressure come with a significant cost [27] and catalyst recycling remains a concern [28]. Enzymes have also been explored for lignin depolymerization, motivated by the overall conversion efficiency of natural

§ *Sandia National Laboratories, Livermore, CA and Albuquerque, NM 87185*
† *Deconstruction Division, Joint BioEnergy Institute, Emeryville, CA 94608*
**Biological Systems and Engineering Division, Lawrence Berkeley National Laboratory, Berkeley, CA 94720*

Electronic Supplementary Information (ESI) available: [details of any supplementary information available should be included here]. See DOI: 10.1039/x0xx00000x

lignocellulose breakdown processes, but so far have resulted in very low monomer yields and are also plagued by repolymerization of the breakdown products [29-34]. Thus, there remains a need for economical high yield depolymerization strategies for condensed lignins that result from carbohydrate-first pretreatment processes.

Toward that goal, we report an alternative method to efficiently cleave C-C bonds and depolymerize lignins at or near room temperature. The method combines sulfonation with a chelator-mediated Fenton (CMF) reaction. Prior work has shown that the Fenton reaction can depolymerize sulfonated polyethylene [35], sulfonated polystyrene [36, 37], and lignosulfonate (LS) [38]. In the work of Areskogh, et al. [38] the emphasis was on increasing the molecular weight of LS for polymeric applications, in contrast to the aim of the present work to depolymerize LS. However, that work also showed that depolymerization of LS occurs at low concentrations of LS for some reaction conditions. Here we focus on optimizing CMF for depolymerization of sulfonated lignins. While our interest in this work is valorizing lignin, we also report depolymerization of polystyrene sulfonate (PSS) because i) PSS has only C-C bonds in the backbone and therefore depolymerization unambiguously occurs through C-C bond cleavage, ii) the narrow molecular weight distribution of PSS standards facilitates establishing trends with reaction conditions, and iii) comparison between results for PSS and LS provides important insights into reaction mechanisms. We first report trends in the molecular weight distribution of PSS with reaction conditions and show that repolymerization can be minimized through control of reagent concentrations and reaction temperature. Then we report depolymerization of LS, showing similar trends in the molecular weight distribution with reaction conditions as for PSS. This depolymerization approach involving hydroxyl radical is non selective [31], and generates a broad distribution of products. Characterization by nuclear magnetic resonance (NMR) and Fourier Transform Infrared (FTIR) spectroscopy indicates that the LS depolymerization products are rich in acid, aldehyde, and alcohol functionalities but are devoid of aromatic groups and aliphatic dienes. In anticipation of a biological conversion approach to upgrade the breakdown products, we report initial studies of growth of a panel of microorganisms on the LS breakdown stream.

2. Experimental Section

2.1 Materials

Polystyrene sulfonate standards were obtained from Scientific Polymer Products (M_w = 5,600 g/mol, PDI 1.02 and 5,200 g/mol, PDI 1.13) and Polymer Standards Service (63,900, PDI < 1.2). A standard purified sodium lignosulfonate sample produced under strong acidic conditions was supplied from a commercial supplier. $FeCl_3$ heptahydrate and 1,2 dihydroxybenzene (DHB) from Aldrich and H_2O_2 (33-37%) from Fisher were used as received. D_2O (99.9%) was purchased from Sigma. Peroxide test strips obtained from MQuant were used to monitor the progress of the CMF reactions.

2.2 Depolymerization of polystyrene sulfonate and lignosulfonate with CMF

CMF reactions with PSS and LS were performed in 10ml glass vials. Aliquots of stock solutions of $FeCl_3$ and DHB were added along with Millipore water to a 10 ml glass vial containing PSS or LS powder to achieve the desired concentrations of substrate and reagents. The pH was adjusted to 6 using NaOH. The reaction was initiated by addition of H_2O_2 and the mixture was stirred with a magnetic stir bar. Peroxide test strips were used to monitor the progress of the reaction by the decrease in H_2O_2 concentration ([H2O2]). During the reaction the pH decreased and was periodically adjusted back to 6.0 using NaOH. Periodically increasing the pH to 6.0 was required for full dissipation of the H_2O_2. Reactions were considered completed when the H_2O_2 was reduced to less than 10% of the initial value. The accuracy of the peroxide test strips was validated using serial dilutions of the H_2O_2 in Millipore water.

Size Exclusion Chromatography (SEC). Molecular weight distributions were determined using an Agilent 1260 HPLC system with PL Aquagel-PH30 and PL Aquagel-OH 50 columns in series and UV detection at 210 nm and 270 nm. Samples were diluted to 1-5 mg/ml by addition of water as needed to avoid detector saturation. The solutions were centrifuged prior to injecting into the HPLC system. The HPLC system contained an in-line filter in front of the analysis column and guard column. The eluant was 1 mM phosphate buffer at pH 9. Polystyrene sulfonate standards were used for calibration.

FTIR. Samples for FTIR analysis were prepared by evaporating reaction liquids onto Teflon substrates and then drying the films in vacuum. IR spectra were collected with a Bruker LUMOS ATR-FTIR microscope using a germanium probe tip contacting the film. For each sample three spectra were collected and averaged. Each spectrum consisted of 16 averaged scans at a resolution of 4 cm^{-1}. Spectra were referenced to a background spectrum collected with no sample present and an atmospheric correction was applied to remove vapor contributions from water and CO_2.

NMR. Samples for analysis by NMR spectroscopy were prepared by first lyophilizing the reaction products and then dissolving 50-100 mg of the dried powder in 700 µl of D_2O. The 1D ^{13}C NMR spectra, 2D ^{1}H-^{13}C heteronuclear single quantum correlation (HSQC) NMR spectra, and ^{1}H-^{13}C Insensitive Nuclei Enhancement by Polarization Transfer (INEPT) NMR spectra were collected using a Bruker-Avance III 600 MHz spectrometer using a 5 mm broadband probes at a sample temperature of 50 ^{o}C. The single pulse inverse gated Bloch decay ^{13}C NMR spectra were collected using WALTZ16 ^{1}H decoupling, and a recycle delay of 60 s. For the 2D HSQC NMR experiments a 5 mm broadband inverse detected probe was used with the Bruker standard pulse program hsqcetgsp.2 which incorporates an echo/anti-echo TPPI acquisition scheme with gradient selection, and shaped inversion pulses on the ^{13}C channel. Spectral widths were 8000 Hz and 25,000 Hz for ^{1}H and ^{13}C, respectively. Signal averaging of 128 scans per t_1 increment was performed in the observe dimension with 256 t_1 time increments recorded, using a recycle delay of 1.5 s. The ^{1}H-^{13}C INEPT NMR spectra were obtained using standard pulse sequences and optimized for a J(CH) = 150 Hz. The ^{1}H chemical shift was referenced to the residual proton signal of the D_2O solvent (δ = + 4.8 ppm) with respect to tetramethylsilane (TMS) (δ =

0.0 ppm), while the ^{13}C NMR chemical shifts were referenced to an external TMS reference (δ = 0.0 ppm).

High Pressure Liquid Chromatography (HPLC). Sugars and acids were quantified by HPLC using an Agilent 1200 series instrument with an Aminex HPX-87H column and a cation H guard column (Bio-Rad, Hercules, CA) kept at 60 ◦C during analysis. The mobile phase was 4 mM H_2SO_4 at a flow rate of 0.6 mL/min. Compounds were quantified using a calibration curve made with pure standards and a refractive index detector at 35 ◦C.

Total organic carbon (TOC). TOC analysis was performed by Hall Environmental Analysis Laboratory (HallEnvironmental.com). Triplicate samples (100 µL) of each reaction mixture was sent to Hall Environmental Analysis Laboratory for analysis. The samples were diluted with Millipore water as needed (dilution factor ~ 300) to perform the TOC analysis using Standard Method 5310B: Total organic carbon by High-temperature combustion.

2.3 Growth of monocultures on depolymerized LS

The microbial strains used for single-organism cultivations in this study can be accessed at the Joint BioEnergy Institute public registry https://public-registry.jbei.org with the following names and accession numbers: *Corynebacterium glutamicum* (JPUB_018348), *Rhodococcus rhodochrous* (JPUB_009659), *Exophiala alcalophila* (JPUB_009664), *Delftia acidovorans* (JPUB_009661), *Pseudomonas putida* (JPUB_009666), *Rhodococcus jostii* (JPUB_009665), *Bacillus subtilis* (JPUB_018353), *Bacillus amyloliquefaciens* (JPUB_019870), and *Rhodosporidium toruloides* (JPUB_013663).

Tryptic soy broth (Sigma-Aldrich) was prepared as 30 g/L in water and autoclaved at 121 ºC for 20 minutes. A 10x yeast nitrogen base (YNB) medium without amino acids (SIGMA-Aldrich) was prepared according to the manufacturer's specifications and supplemented with Complete Supplement Mixture (CSM, MP Biomedicals, USA) at a final concentration of 80 mg/L. The pH of the resulting medium (YNB+CSM) was adjusted to a value of 6 with 10 N NaOH and the solution was filter sterilized (0.45 µm cellulose-acetate membrane). The depolymerized lignosulfonate material at a concentration of 5 mg/mL was also filtered (0.45 µm cellulose-acetate membrane), mixed at a 9:1 v/v ratio with the 10x YNB+CSM stock solution, and used for microbial cultivations.

To start the cultivations, all organisms were inoculated from agar plates and grown for 24 hours in tryptic soy broth at 30 ºC. The cells were then centrifuged, resuspended in water, and transferred at an initial OD of approximately 0.1 to 1 to 48-well plates containing cultivation medium (500 µL final volume per reaction). The cultivations were performed in triplicate. The plates were covered with an AeraSeal sealing film (Excel Scientific, USA) and a plastic lid to prevent evaporation and incubated at 30 ºC with shaking at 300 rpm for 60 h. Cell density was determined by measuring absorbance at 600 nm with a plate reader (Tecan Spark, Switzerland).

2.4 Assay for melanin production in *E. alcalophila*

Melanin production in *E. alcalophila* cells was quantified by fluorescence using a method adapted from Fernandes et al. [39]. Seed cultures were grown for 24 h in tryptic soy broth, then centrifuged and resuspended in water before transferring the cells to 14 mL round bottom tubes containing 5 mL of medium at an initial OD of 0.1. Culture samples (1.5 mL) were collected at the beginning of the experiment and after incubation at 30 ºC with shaking for 24 h. The cells in these samples were harvested by centrifugation and the consumption of compounds in the supernatants was tracked using a previously reported HPLC method to detect sugars and acids [40]. For melanin analysis, the cell pellets were resuspended in 5 M NaOH containing 10% (v/v) of DMSO. The mixture was incubated for 1 h at 80 ºC with 400 rpm shaking in a Thermomixer R (Eppendorf, Germany) and centrifuged at 3000 x g for 3 minutes. 100 µL of the supernatant were transferred to a clean tube, mixed with 200 µL of 30% H_2O_2, and incubated for 1 h in the dark at room temperature using 1.5 mL tubes with loosely closed caps. At the end of the incubation, samples were briefly centrifuged, mixed with a pipette, and transferred (100 µL) to a 96-well black plate with flat transparent bottom (Corning, USA). Fluorescence was immediately measured at excitation and emission wavelengths of 470 and 550 nm, respectively, using a Tecan Spark plate reader (Tecan, Switzerland). Commercial Sepia melanin (Sigma Aldrich, USA) was subjected to the same treatment and used to generate a calibration curve. Experiments were performed in triplicate.

3. Results

The chemical structure of PSS and a representative chemical structure for LS are given in Figure 1. For PSS, a sulfonic acid group exists at the para position of the aromatic ring whereas in our lignosulfonate sample the sulfonic acid groups are located on the alpha or gamma carbons of the aliphatic chain adjacent to the aromatic ring. For lignosulfonates produced under strongly acidic conditions, as for the sample used in this work, sulfonation occurs mainly on the alpha carbon [41].

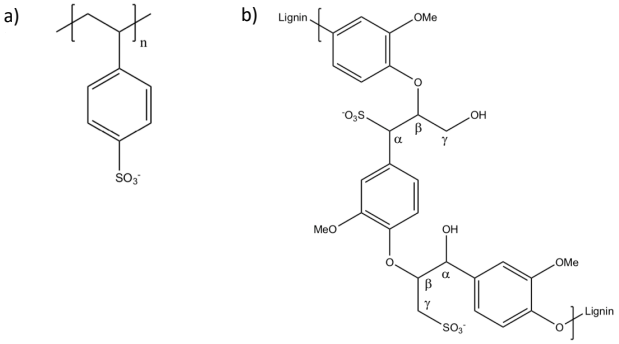

Figure 1. Chemical structures of a) polystyrene sulfonate and b) lignosulfonate

3.1 Depolymerization of PSS

Figure 2 shows the decrease in molecular weight for PSS 67K and PSS 5.2K for CMF reactions with [$FeCl_3$] = [DHB] = 1 mM, and [H_2O_2] = 0.5% at room temperature (RT) using UV detection at 210 nm and 270 nm. The weight averaged molecular weight (M_w) decreases by a factor of 75 for PSS 67K (from 75,000 g/mol to 1,000 g/mol) and by a factor of 4.4 for PSS 5.2K (UV 210). For the two samples the final M_w is comparable at ~ 1000 g/mol which suggests that careful optimization of conditions will be required to depolymerize to M_w values lower than ~ 1000 g/mol. At 210 nm the UV signal of the post

reaction material is decreased relative to the unreacted material whereas at 270 nm the UV signal increased upon reaction. The latter indicates an increase in conjugation within the structures after

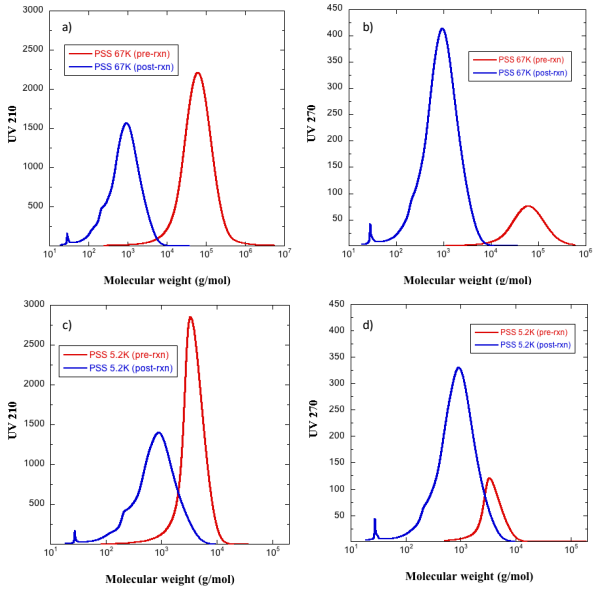

Figure 2. a, b) Molecular weight decrease with CMF reaction for [PSS 67K] = 5 mg/ml at [FeC_3] = [DHB] = 1 mM and [H_2O_2] = 0.5% at RT measured at 210 nm and 270 nm, respectively. c, d) Molecular weight decrease with CMF reaction for [PSS 5.2K] = 5 mg/ml at [FeC_3] = [DHB] = 1 mM and [H_2O_2] = 0.5% at RT measured at 210 nm and 270 nm, respectively.

reaction. The full UV spectra for these samples are given in the supporting information (Figures S1 and S2). Toward the goal of optimizing CMF for depolymerization, the dependencies of M_w on various reaction conditions were determined. Figure 3 shows changes in post-reaction M_w for CMF reactions with PSS5.2K as a function of [$FeCl_3$], [PSS], [H_2O_2], and temperature. The strongest

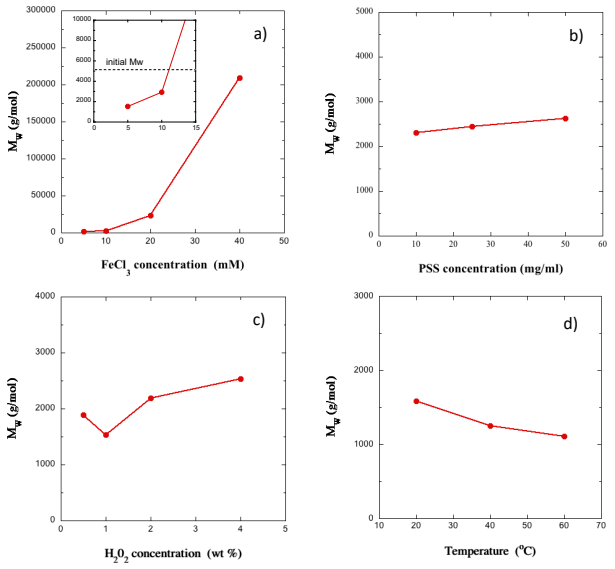

Figure 3. Post-reaction M_w for PSS 5.2K as a function of a) [$FeCl_3$] ([H_2O_2] = 1%), b) [PSS] ([$FeCl_3$] = 10 mM, [H_2O_2] = 1%), c) [H_2O_2] ([$FeCl_3$] = 5 mM), and d) temperature ([$FeCl_3$] = 1 mM, [H_2O_2] = 0.5%). Unless otherwise indicated, [LS] = 5 mg/ml, [DHB] = 4 mM, and temperature = RT.

impact on M_w occurs with [$FeCl_3$], with M_w increasing strongly with [$FeCl_3$] (Fig 3a). Depending on the value of [$FeCl_3$], M_w values greater or less than that of the initial sample can be obtained (Figure 3a inset). These results suggest that both C-C bond cleavage and repolymerization occur, and that repolymerization is minimized at lower [$FeCl_3$]. The inset to Figure 3a shows that the final M_w is lower than the initial value for [$FeCl_3$] < 11 mM for these reaction conditions.

Figure 3b shows that M_w also increases with [PSS], albeit with a much weaker dependence, suggesting that repolymerization is also minimized at lower [PSS]. The trend with [H_2O_2] is more complex as a minimum is observed. We suggest that the minimum is a competition between the following two effects: increasing C-C bond cleavage occurs with increasing [H_2O_2] which alone would lead to decreasing M_w, but at some value of [H_2O_2] repolymerization begins to occur and increases with increasing [H_2O_2] causing an increase in M_w. Finally, Figure 3d shows that M_w decreases slightly with increasing T.

Figure 4 shows the FTIR spectra for depolymerized PSS products for strongly depolymerizing reaction conditions ([H_2O_2] = 1%, [$FeCl_3$] = [DHB] = 1 mM, RT) measured in attenuated total reflection mode after depositing the post reaction solution onto a substrate and drying the film in vacuum. The spectrum of unreacted PSS is also shown for comparison. Band assignments for PSS were made following prior work [42-44]. For PSS strong absorbance at 1184 cm^{-1} and 1042 cm^{-1} correspond to the SO_3^- asymmetric and symmetric stretch vibrations, respectively, and bands at 1130 cm^{-1} and 1010 cm^{-1} correspond to the in-plane skeletal vibration and in-plane bending vibrations, respectively, of the substituted benzene ring. The band at

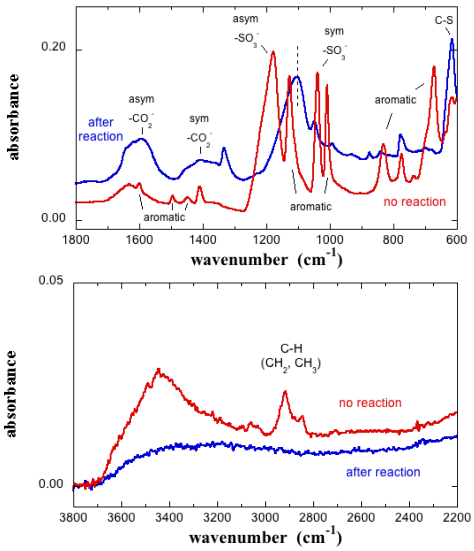

Figure 4. FTIR spectra for PSS 5.2K and after reaction with [$FeCl_3$] = [DHB] = 1 mM , [H_2O_2] = 1% at RT.

833 cm^{-1} is due to CH out-of-plane vibration for para disubstituted benzene. The band at 672 cm^{-1} is due to aromatic ring vibration involving C-S stretching. Weaker aromatic skeletal vibrations are present at 1598 cm^{-1}, 1514 cm^{-1}, and 1425 cm^{-1} in unreacted PSS. The band at 1460 cm^{-1} is assigned to C-H deformation combined with aromatic ring vibration. Bands at 2800-3000 cm^{-1} are due to the C-H stretch of methyl and methylene groups.

In the post reaction IR spectrum, the aromatic bands are strongly reduced. The broad band centered at 1600 cm^{-1} in the post reaction sample is attributed to the asymmetric stretch of a carboxylate anion that is associated with Fe or Na cations. Whereas free carbonyl

occurs at 1700-1720 cm^{-1}, the band shifts to 1600 cm^{-1} upon association with a cation in a dried salt, as shown in a prior study of malic acid and sodium malate [45]. The broad band centered at 1400 cm^{-1} in the post reaction sample is attributed to the symmetric carboxylate C-O vibration [45]. Bands at 2800-3000 cm^{-1} due to the C-H stretch of methyl and methylene groups are absent in the post reaction sample. Methylene groups are present in the backbone of PSS, and their absence in the post reaction sample is consistent with extensive oxidative and /or cleavage of backbone C-C bonds. We tentatively assign the strong band at 1100 cm^{-1} in the post reaction sample to C-O stretch of tertiary alcohols, esters, or aliphatic ethers generated upon oxidative cleavage of C-C bonds.

3.2 Depolymerization of LS

Figure 5 displays the decrease in molecular weight for CMF reactions of LS with [$FeCl_3$] = [DHB] = 0.5 mM, and [H_2O_2] = 0.5% at 22 °C using UV detection at 210 nm and 270 nm. M_w decreased by a factor of > 10 (from 28,000 g/mol to 2700 g/mol, UV 210 nm) and M_w/M_n

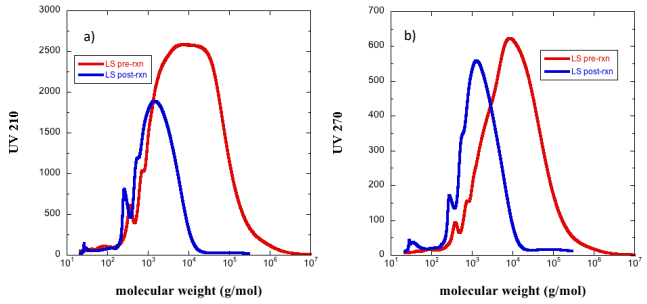

Figure 5. Molecular weight distribution for [LS] = 5 mg/ml before and after reaction with [$FeCl_3$] = [DHB] = 0.5 mM and [H_2O_2] = 0.5% at RT measured at a) 210 nm and b) 270 nm.

decreased from 29 to 5 (UV 210 nm). The UV signals at 210 nm and 270 nm both decrease upon reaction. The latter is in contrast with the results for PSS in Figure 2b and Figure 2d where the absorbance at 270 nm increased after CMF reaction. The full UV spectra for these samples are given in the supporting information (Figure S3). In Figure 5a a single low molecular weight peak is resolved at 280 g/mol, a shoulder occurs at ~500 g/mol, and the peak of the distribution occurs at 1400 g/mol.

Figure 6 shows the variation in post reaction M_w for CMF reactions with LS as a function of [$FeCl_3$], [LS], [H_2O_2], and temperature. As for PSS, by far the strongest effect on M_w occurs with [$FeCl_3$], with M_w increasing strongly with [$FeCl_3$] (Fig 6a). The results show that M_w can be increased or decreased substantially depending on [$FeCl_3$]. Figure 6b shows that M_w also increases with [LS], suggesting that repolymerization is minimized at lower [LS]. The trend of increasing M_w with [LS] is consistent with prior reports for the Fenton reaction with LS [38] and for alkali-O_2 oxidation of soda lignin [46]. Figure 6c shows that very little variation in final M_w occurs with [H_2O_2] from 1 % to 4 % for strongly depolymerizing conditions, but the final M_w was slightly greater at [H_2O_2] = 0.5 %. As for the PSS reactions, we suggest that the amount of H_2O_2 is limiting at 0.5% resulting in a decrease in the number of C-C backbone bonds cleaved. Figure 6d shows that for strongly depolymerizing conditions, the final M_w decreases only slightly with increasing T. While the effects of [LS], [H_2O_2], and T are weaker than for [$FeCl_3$], they are important for achieving the lowest possible M_w by minimizing repolymerization.

While the present work is focused on depolymerization, we note that increasing the molecular weight of LS is important for certain

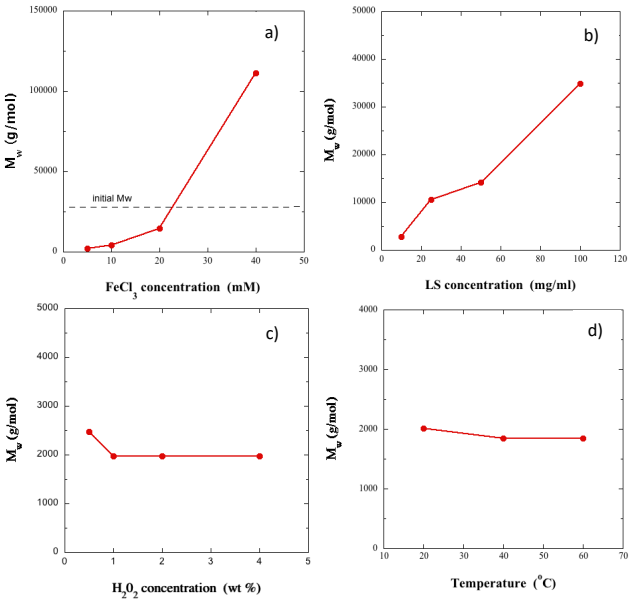

Figure 6. Post-reaction M_w for LS as a function of a) [$FeCl_3$] ([H_2O_2] = 1%), b) [LS] ([$FeCl_3$] = 10 mM, [H_2O_2] = 1%), c) [H_2O_2] ([$FeCl_3$,] = 5 mM), and d) temperature ([$FeCl_3$] = 1 mM, [H_2O_2] = 0.5%). Unless otherwise indicated, [LS] = 5 mg/ml, [DHB] = 4 mM, and temperature = RT.

polymer applications, such as its use as a concrete plasticizer [38, 46]. The molecular weight distributions for the highest M_w in Figure 6a and Figure 6b are shown in Figure S4 in the supporting information. Figure 6a shows that CMF at high [Fe] is a highly effective method to increase M_w. Iron is a relatively low-cost reagent, especially in the

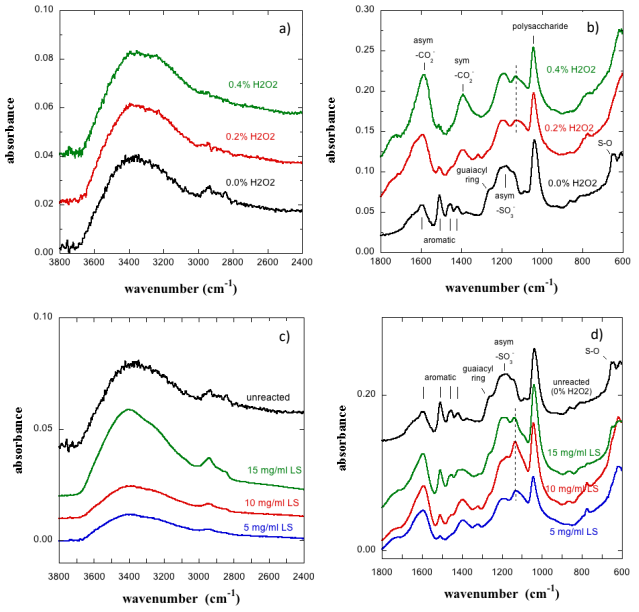

Figure 7. a, b) FTIR spectra for LS as a function of [H_2O_2] with [LS] = 5 mg/ml, and c, d) as a function of [LS] with [H_2O_2] = 0.5%. Reactions were performed with [$FeCl_3$] = [DHB] = 0.5 mM at 40 °C.

form of iron sulfate which can be used in place of $FeCl_3$ in the CMF reaction.

FTIR spectra are given in Figure 7a and Figure 7b for LS depolymerization products from a series of reactions conducted as a function of [H_2O_2] (a and b), and as a function of [LS] (c and d). The spectrum of unreacted LS is also shown for comparison. Band

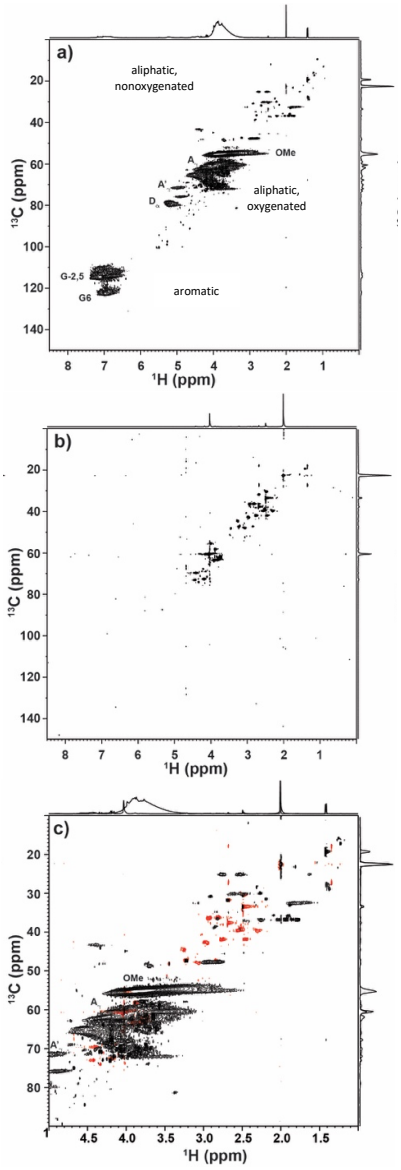

Figure 8. Two dimensional ^{1}H-^{13}C HSQC NMR spectra for a) LS and b) depolymerization products for CMF reaction of LS with [$FeCl_3$] = 1 mM, [DHB] = 10 mM, [H_2O_2] = 1% at 40 °C. The aliphatic region is expanded and overlayed for the two samples in c), with the post-reaction spectra shown in red.

assignments for LS were made based on prior work [47, 48]. Bands at 2800-3000 cm^{-1}, 1540 cm^{-1}, 1460 cm^{-1}, and 1420 cm^{-1} are assigned as for PSS. The band at 1050 cm^{-1}, which is largely unaffected by the CMF reaction, is assigned to polysaccharide (C-O and C-C stretching and C-OH bending). The band at 1260 cm^{-1} is assigned to guaiacyl ring vibration. The broad band at 1190 cm^{-1} is assigned to the SO_3^- asymmetric stretch vibration. The SO_3^- symmetric stretch vibration expected at 1040 cm^{-1} apparently overlaps with the polysaccharide band. The band at 640 cm^{-1} is assigned to S-O stretch of the sulfonic acid groups. As in the case of CMF reactions with PSS, for LS the aromatic vibrations at 1514 cm^{-1}, 1469 cm^{-1}, and 1420 cm^{-1} are reduced substantially in the post reaction spectrum and strong bands from symmetric and asymmetric stretch of carboxylate anion centered at 1600 cm^{-1} and at 1400 cm^{-1} are present in the post reaction spectra. Bands at 2800-3000 cm^{-1} for unreacted LS due to the C-H stretch of methyl and methylene groups are reduced in the post reaction spectra. Methoxy groups in unreacted LS are the likely source of these bands. Their absence in the post reaction sample is consistent with oxidation of methoxy groups to generate methanol which is evaporated during sample drying. Oxidation of methoxy groups to generate methanol has been reported previously for oxidative treatments of lignin [49-51]. A band at 1130-1135 cm^{-1} is present in the post reaction spectra, which is not present in unreacted LS. We tentatively assign that band to the C-O stretch of secondary or tertiary alcohols generated upon oxidative cleavage of C-C bonds.

Two-dimensional ^{1}H-^{13}C HSQC NMR spectra for LS in D_2O before and after the CMF reaction is shown in Figure 8a and Figure 8b, respectively. The spectrum before reaction contains signals characteristic of guaiacyl groups (δ^{13}C = 110 to 120 ppm) but shows little syringyl content (δ^{13}C = 105 to 108 ppm) [52]. Strong signals are observed for methoxy groups (δ^1H ~3.5-4.0 ppm, δ^{13}C ~ 55 ppm) and for A type β-O-4 ethers (A_b: δ^1H ~5.1-5.4 ppm, δ^{13}C ~ 78 - 80 ppm; A_a: δ^1H ~4.5-4.7 ppm, δ^{13}C ~ 66 ppm) [52]. For the post reaction sample the 2D HSQC NMR spectrum is entirely devoid of aromatic signals. This is also supported by the lack of aromatic signal δ^{13}C = 100 to 120 ppm in the 1D NMR spectrum (see below). The aliphatic region of the spectrum indicates a nearly complete elimination of methoxy groups and β-O-4 ether linkages. The majority of the signals have not been assigned, although weak signals for ethanediol are assigned (δ^1H ~1.35 ppm, δ^{13}C ~ 22 ppm; δ^1H ~5.3 ppm, δ^{13}C ~ 88 ppm) following a prior study [6]. Signals corresponding to methanediol, acetic acid, and acetaldehyde [6] were not detected.

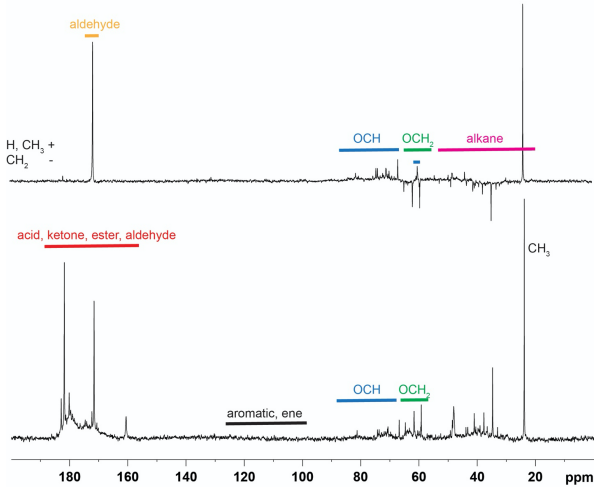

Figure 9. INEPT NMR spectra (top) and quantitative ^{13}C NMR (bottom) for depolymerization products of CMF reaction of LS with [$FeCl_3$] = 1 mM, [DHB] = 10 mM, and [H_2O_2] = 1% at 40 °C.

Quantitative 1D ^{13}C NMR and ^{1}H-^{13}C Insensitive Nuclei Enhancement by Polarization Transfer (INEPT) NMR spectra for LS in D_2O after CMF reaction are given in Figure 9. Integration of the ^{13}C NMR spectra over the ranges 200 to 150 ppm (carbonyls, 56%), 150-

100 ppm (aromatics and alkenes, 0%), and 90-65 ppm (oxygenated carbons, ethers, alcohols, esters, and alkanes, 8%) and 65 – 0 ppm (alkanes, 36%) indicates that the majority of carbon environments are carbonyls. The very low diene content indicates that virtually no muconic acid-type structures are present, in contrast to the case of milder oxidizing treatments [53]. The ^{1}H-^{13}C INEPT NMR spectrum indicates whether the number of protons bonded to each C environment is odd (CH_3, CH positive) or even (CH_2 negative). These data indicate that the ^{13}C signal at 171.6 ppm is from aldehyde as it has a direct CH coupling, while the remainder of the ^{13}C resonance in this region are not observed in the INEPT sequence (*i.e.* no CH bonds) and must therefore arise from a carbonyl environment in an acid, ester or ketone species. Integration of that region in the ^{13}C NMR spectrum indicates that ~9% of the C are aldehydes.

depolymerization products alone and with 0.2% glucose. For these assays, 5 g of LS in 1 liter water were depolymerized with [$FeCl_3$] = 1 mM, [DHB] = 13 mM, [H_2O_2] = 1.2% at 40 °C. The molecular weight distribution the resultant depolymerized material is shown in Figure S6. The M_w and Mw/Mn were 770 g/mol and 3.6, respectively. Based on integrating the area under the curve in Figure S6 5% was resolved as a peak at 250 g/mol, 8% was resolved as a peak at 500 g/mol, and 39% of the material had molecular weight < 1000 g/mol.

Figure 10 shows OD600 for monocultures of the panel of microorganisms in microliter plates growing on 5 mg/mL LS depolymerization products alone and supplemented with 0.2% glucose (Glc). Also shown are the OD600 values obtained for 0.2% glucose alone and for the base medium (YNB+CSM) that was added to all conditions. The results show that several organisms can grow

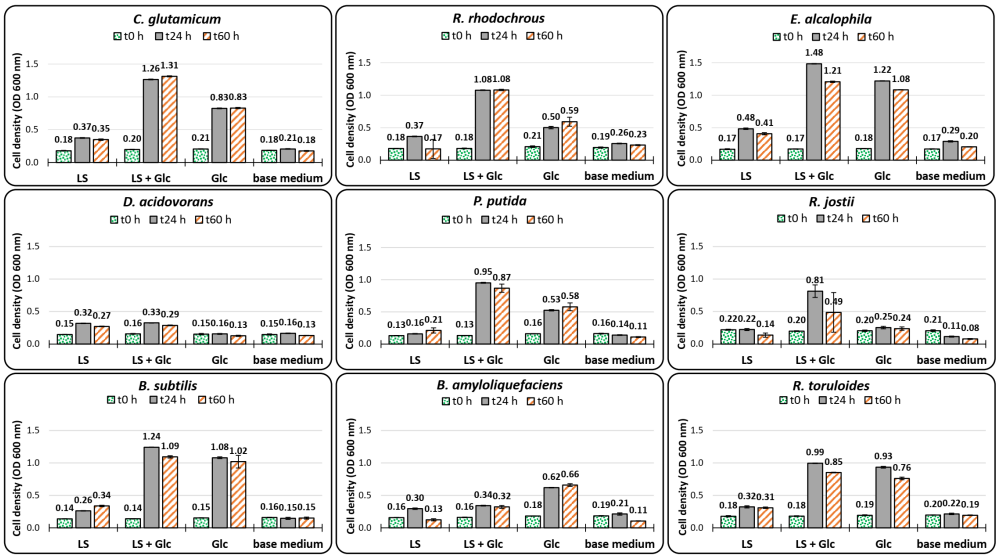

Figure 10. Growth of monocultures in the LS breakdown stream or base medium in the presence or absence of glucose. Bars represent the average of three replicates and the error bars indicate the standard deviation.

To estimate the amount of material lost as CO_2 or other low molecular weight volatile species such as methanol and formaldehyde during the CMF reaction, samples of the post reaction solution were freeze-dried and then weighed and compared to the total mass of LS, DHB, and $FeCl_3$ added to the reaction mixture. For comparison, unreacted LS was dissolved in water and then freeze-dried and weighed in the same manner. For unreacted LS, the mass recovered after freeze-drying was 89 +/- 3% and for the post CMF reaction samples ([LS] = 5 mg/ml, [$FeCl_3$] = [DHB] = 0.5 mM, [H_2O_2] = 0.5%, at 40 °C) the mass recovered after freeze-drying was 91 +/- 3%. This suggests that the mass of carbon lost as CO_2 is small. However, a precise determination of carbon lost is not possible by this method since the mass of oxygen added to the LS breakdown products during the CMF reaction is unknown. Total organic carbon (TOC) measurements were also performed for products of reactions with varying [H_2O_2] for [LS] = 5 mg/ml, [$FeCl_3$] = [DHB] = 0.5 mM at 40 °C. The results, shown in Supporting Information Figure S5, indicate < 20% loss of TOC at [H_2O_2] = 0.5%.

3.3 Growth of organisms on the products of LS depolymerization

The depolymerization products were screened for bioavailability by measuring the growth of a panel of microorganisms on the LS on the LS material, alone or in combination with glucose. These reach maximum cell density within 24 h. However, different growth profiles were observed. For example, the simultaneous presence of LS and glucose resulted in an additive effect in *E. alcalophila*, and *B. subtilis and R. toruloides*, while a synergistic effect (higher OD than the sum of the values obtained with only LS or glucose) was observed with *C. glutamicum*, *R. rhodochrous*, *P. putida* and *R. jostii*. Growth with only LS was modest but reproducible, indicating that some components in the depolymerized stream can be consumed. The substantial growth with LS + glucose suggests that the LS material imposes low toxicity to these organisms and that there may be compounds in the breakdown stream that can be assimilated but cannot sustain growth without an additional carbon or energy source such as glucose. Other interesting effects were observed with *D. acidovorans* and *R. jostii. D. acidovorans*, which is known to be unable to metabolize glucose grew noticeably on depolymerized LS. *R. jostii* only grew in presence of both LS and glucose.

Finally, we assayed for melanin production in *E. alcalophila* in the presence of 0.2% glucose with and without addition of depolymerized LS. *E. alcalophila* produces melanin from malonyl-CoA through the constitutively expressed 1,8-dihydroxynaphtalene (DHN) pathway [54]. Melanin production was measured with a

fluorescence method described in the Methods section. The results shown in Figure 11 indicate nearly twice as much melanin was produced in the presence of depolymerized LS compared with glucose alone. This strongly suggests that some components of the depolymerized LS stream are being utilized by *E. alcalophila*. HPLC data (SI Figure S7) shows a decrease in organic acids content following incubation of *E. alcalophila* on depolymerized LS for 24 h, suggesting that *E. alcalophila* utilizes organic acids in the depolymerized LS.

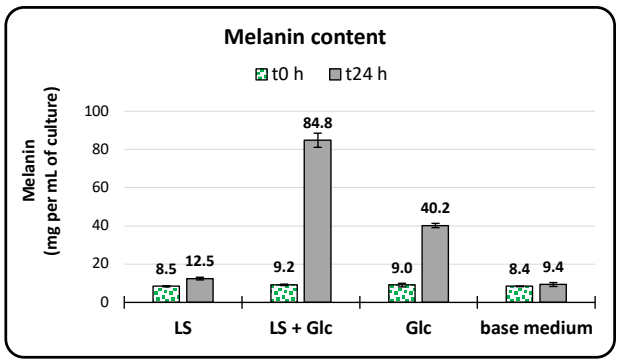

Figure 11. Production of melanin in *E. alcalophila* grown on glucose, depolymerized LS, glucose + depolymerized LS, and base medium. More than twice the melanin was produced when depolymerized LS was included along with glucose. Bars represent the average of three replicates and the error bars indicate the standard deviation.

4. Discussion

Cleaving C-C bonds is essential to achieve high yield depolymerization of natural lignins. Cleaving C-C bonds generally requires high temperatures. However, some specific enzymes, such as aldolases [55] and β-diketone hydrolases [56] perform this feat at room temperature by creating a local environment that drastically lowers the energy barrier for bond cleavage. Nonspecific oxidative enzymes such as lignin peroxidase can also cleave C-C bonds at ambient conditions [57-59], but the process is very inefficient. Here we report a method to cleave C-C bonds efficiently in polymers containing sulfonic acid groups at or near room temperature. Depolymerization of PSS by CMF shows unambiguously that C-C backbone bonds are cleaved under mild conditions using this method. Depolymerization of sulfonated PE, PSS, and LS by Fenton reactions has been demonstrated in prior work [35-38]. In the present work we show that depolymerization of PSS and LS proceeds efficiently with CMF reactions that were optimized to use low amounts of H_2O_2 and we demonstrate bioavailability of some of the products. The molecular weight distribution of LS depolymerized by CMF does not contain as many resolved low molecular weight peaks as is typically reported for other depolymerization methods [9, 15, 30, 60]. We expect that cleaving C-C bonds nonspecifically in the present approach results in a larger range of breakdown products and a more continuous molecular weight distribution than occurs with methods that cleave mainly ether bonds.

At low reaction severity depolymerization occurs for both PSS and LS, and the trends of M_w with reaction conditions are similar for the two sulfonated polymers even though the chemical structures of these polymers differ greatly. In particular, the location of sulfonation is entirely different in LS and PSS, with sulfonation occurring on aromatic rings in PSS and on aliphatic OH groups in the LS sample. Sulfonation appears to be a requirement for efficient backbone C-C bond cleavage by CMF, as CMF reaction with lignin in absence of sulfonation results in aromatic ring opening but little decrease in molecular weight for these conditions [61]. The presence of aromatic groups is not required for C-C bond cleavage in sulfonated polymers by the Fenton reaction, as sulfonated polyethylene can also be depolymerized with this method [35]. Together, these findings suggest that the positively-charged Fe ions, alone or in complex with DHB, associate strongly with negatively-charged sulfonic acid groups such that hydroxyl radical is generated in very close proximity to the polymer chain. Hydroxyl radicals are highly reactive and are believed to react within 1-5 molecular diameters of their site of formation in the crowded environment of living cells [62]. We suggest that generating hydroxyl radical near a lignin chain greatly increases the probability of a productive reaction.

The strength of the sulfonic acid group seems to be critical for effective C-C bond cleavage using CMF. Lignin (absent sulfonation) is known to chelate Fe through interaction with hydroxy groups [50, 63], however CMF reaction does not lead to extensive depolymerization in that case. We propose that the efficient and extensive C-C bond cleavage for CMF with polymers functionalized with SO_3H is due to strong electrostatic interactions between positively charged Fe ions and negatively charged sulfonic acid groups that occurs in the pH range > 2, generating intensive interactions of hydroxyl radicals with the polymer chains.

The role of DHB in the CMF reactions reported here is somewhat enigmatic. Since the reaction of Fe(III) with H_2O_2 is 3 orders of magnitude slower than that of Fe(II) with H_2O_2 [64], Fe chelators such as DHB that efficiently reduce Fe(III) to Fe(II) have been used [65-67], motivated by the mechanism for degrading wood by brown rot fungi [68, 69]. The coordination number of complexes of Fe and DHB is pH dependent, and only monocomplexes can reduce Fe(III) [64, 70]. Whereas the rate of the Fenton reaction is greatest at low pH (2-3), the use of DHB or other Fe-chelators increases the pH range for reactivity of Fenton systems to pH > 5 [64, 66, 70, 71]. Catecholates have been reported to reduce 5-6 moles of Fe(III) per mole of chelator [71]. Most of the CMF reactions in the present work involved 0.5-1.0% H_2O_2 (147 mM to 294 mM). Since DHB was added at only 4 mM (Figure 3 and Figure 6), the amount of H_2O_2 consumed is far greater than can be accounted for if H_2O_2 reacts only with Fe(II) and if Fe(III) is only reduced to Fe(II) by DHB. We conclude that oxidized LS and oxidized PSS have substantial Fe(III)-reducing capability, in agreement with prior work [50].

Achieving the maximum reduction in M_w requires careful moderation of the reaction conditions. Our data show that repolymerization occurs with increasing reaction intensity (higher [$FeCl_3$] and [H_2O_2]) and with increasing concentration of LS. Higher reaction intensity will result in a greater density of lignin fragments that contain radicals, therefore increasing the prevalence of

condensation reactions. With increasing [LS] the probability that lignin fragments containing radicals come into contact before the radicals dissipate increases.

To quantitatively evaluate the efficiency of ring-opening and backbone bond cleavage reactions with respect to H_2O_2 consumption, we consider the case of M_w reduction in PSS 67K by a factor of 75 in Figure 2a and Figure 2b, achieved with 0.5% H_2O_2 (147 mM). Since 5 mg/ml PSS corresponds to 27 mM monomer, and since one hydroxyl radical is generated for each molecule of H_2O_2 that reacts in the Fenton reaction, 27 mM H_2O_2 is the stoichiometric requirement for opening all the aromatic rings, assuming a single hydroxyl radical is sufficient to open an aromatic ring. For reduction in M_w by a factor of 75 we estimate at least 64 backbone bonds per chain must be cleaved on average. A chain of 67K has 366 monomers and so backbone bonds must be cleaved in 17% of the monomers (64/366 ~ 0.17). Therefore, we estimate that the stoichiometric amount of H_2O_2 required to cleave the backbone bonds is ~ 5 mM H_2O_2 (0.17 x 27 mM monomers), again assuming that a single hydroxyl radical is sufficient to cleave a backbone C-C bond). Assuming that repolymerization is negligible at 0.5% H_2O_2 we estimate that the amount of H_2O_2 consumed was at most a factor of 4.5 (147 mM/(27mm + 5mM)) greater than the stoichiometric requirement. We consider this value to be an upper limit as we expect that more than one hydroxyl radical is required to open a single aromatic ring and or to cleave a single backbone C-C bond. Further study into the mechanism is required to determine if indeed a single hydroxyl radical is sufficient to open a single aromatic ring and or to cleave a single backbone C-C bond, but we consider the factor of 4.5 to indicate an efficient reaction with respect to H_2O_2 consumption.

Abdelaziz et al. recently reported oxidative depolymerization of LS using heterogeneous catalysts at elevated temperature and pressure [6], which invites comparisons with the present approach. Regarding the extent of depolymerization, they reported a shift from a very broad distribution with peak molecular weight (M_p) ~ 3000 g/mol to a much narrower distribution with M_p = 1400 g/mol (UV detection at 280 nm). The present work (Figure 5b) shows a decrease from M_p = 9000 g/mol to M_p = 1300 g/mol and the lowest M_p achieved in the present work for this LS sample is 850 g/mol. This comparison suggests that repolymerization may be more readily minimized using the present method. In agreement with the present work, the products reported by Abdelaziz et al. were mostly de-aromatized, and a strong loss of methoxy groups was also observed. Abdelaziz et al. reported that the low molecular weight products methanol (δ^1H ~ 3.35-3.45 ppm, δ^{13}C ~ 48-50 ppm), acetaldehyde (δ^1H ~ 2.20-2.30 ppm, δ^{13}C ~ 30 ppm), 1,1-ethanediol (δ^1H ~ 1.32 ppm, δ^{13}C ~ 23 ppm; δ^1H ~ 5.25 ppm, δ^{13}C ~ 88 ppm), methanediol (δ^1H ~ 4.85 ppm, δ^{13}C ~ 82 ppm), and acetic acid (δ^1H ~ 2.08-2.25 ppm, δ^{13}C ~ 20-21 ppm) were present in the reaction products. Larger compounds identified as reaction products included polyhydroxylated carbonyl-containing aliphatic ring compounds such as β-hydroxy-γ-butyrolactone (δ^1H ~ 3.95 ppm, δ^{13}C ~ 62.5 ppm; δ^1H ~ 4.35 ppm, δ^{13}C ~ 77 ppm; δ^1H ~ 4.55 ppm, δ^{13}C ~ 77 ppm) and (tentatively) the β-sulphonate derivative of γ-butyrolactone (δ^1H ~ 2.85-2.95 ppm, δ^{13}C ~ 31 ppm; δ^1H ~ 3.10-3.20 ppm, δ^{13}C ~ 31 ppm; δ^1H ~ 4.0 ppm, δ^{13}C ~ 54 ppm; δ^1H ~ 4.7 ppm, δ^{13}C ~ 69 ppm). Despite the fact that the aromatic signal in the 2D ^{1}H-^{13}C HSQC NMR spectrum was strongly decreased, low levels of the aromatic monomers vanillin, p-hydroxybenzaldehyde, vanillic acid, and p-benzoic acid were detected by supercritical fluid chromatography mass spectrometry following extraction with ethyl acetate and subsequent concentration. The lactones detected by Abdelaziz et al. were not detected by ^{1}H-^{13}C HSQC NMR in the breakdown stream in the present work. Opening of aromatic rings should lead to muconic acid structures and these form lactones via ring closure for neutral or acidic conditions [46, 72]. Since we observed virtually no diene structures in our product stream and we did not observe the lactones detected by Abdelaziz et al., we suggest that hydroxyl radicals or other species react rapidly with the dienes before ring closure and lactone formation can occur. The fact that the low M_w compounds methanol, methanediol, acetaldehyde, and acetic acid were identified in the reaction products of Abdelaziz, et al. but were not detected in the present work may be due to the fact that in the present work the samples were freeze-dried prior to dissolving in D_2O for NMR analysis, whereas the reaction mixtures were added directly to D_2O for NMR analysis in the work of Abdelaziz and co-worker. Many other differences exist in the ^{1}H-^{13}C HSQC NMR signals for the two product streams indicating that the reaction pathways are substantially different.

Most prior work on biological conversion of lignin has focused on releasing aromatic monomers and dimers from lignins and utilizing conversion hosts with suitable native or engineered metabolic pathways to convert the aromatic compounds into useful chemicals or intermediates [4-9]. This is motivated by natural processes of lignin depolymerization and utilization in the environment. While this occurs very slowly in nature, as an industrial process this approach is most promising for engineered lignins that contain a very high content of ether bonds [11]. For natural lignins this approach has had limited success due to several factors including low yield of aromatic monomers, toxicity of some of the aromatic breakdown products, and the tendency for polymerization to occur simultaneous with depolymerization. The yield of aromatic monomers is fundamentally limited by the presence of C-C bonds.

In this work we introduce an alternative, or complementary, approach. We have shown that CMF reaction with sulfonated lignin cleaves C-C bonds efficiently at or near room temperature at ambient pressure. We also show that under suitable conditions repolymerization can be minimized. These reaction conditions open the aromatic rings and the breakdown products consist of low molecular weight species rich in acid, aldehyde, and alcohol groups. While our data for growth of a panel of monocultures on the LS breakdown stream shows encouraging evidence of its utilization, especially in the presence of a small amount of glucose, it remains to be seen whether robust microbial hosts can be found, evolved, or engineered to efficiently utilize a high fraction of this diverse stream of breakdown products, and whether the carbon can be efficiently funneled into pathways that produce a high yield of useful chemicals or intermediates. Another question for further research is whether the chemical nature of the breakdown products can be tailored with reaction conditions. Our work suggests that organic acids are being taken up and consumed by the microbial hosts (Fig S6). We expect that generating more acids and less aldehydes will lead to greater biological utilization. Further decrease in M_w is also likely to be possible with further optimization of reaction conditions.

While many questions remain to be answered for this approach, we offer some preliminary comments regarding economics. One key factor is the ratio of low molecular weight products generated per amount of H_2O_2 consumed during depolymerization. In our present work with LS, to achieve 100% conversion from M_w = 28,000 to M_w = 950 g/mol one gram of H_2O_2 (pure basis) was consumed per 0.44 g of LS and to achieve M_w = 770 g/mol one gram of H_2O_2 was consumed per 0.30 g of LS ([$FeCl_3$] = [DHB] = 0.5 mM, T= 40 °C). These values do not seem prohibitive, and higher yields will likely result with further optimization. Another concern is the amount of carbon lost as CO_2 in the process. We established an upper bound of 20 % of the original carbon that was lost as CO_2 or other volatile compounds such as methanol or formaldehyde. Considering that ~10% of the carbon is in the form of methanol from oxidation of methoxy groups, we conclude that very little carbon is lost as CO_2 in this process. Whereas a large amount of relatively low-cost LS is currently available from the pulp and paper industry, a far greater amount of kraft lignin is available. To utilize this process with kraft lignin and lignin from a lignocellulosic biorefinery, the lignins would need to be sulfonated, adding to the process cost. Another factor impacting the economics of the process is the rate of throughput. The results in Figure 3 and Figure 6 indicate that repolymerization of fragments after C-C bond cleavage are minimized at low [Fe] and low [LS], but these conditions will lower the rate of reaction and throughput. However, based on our results we estimate that 5 mg/ml LS can be depolymerized from 28,000 g/mol to roughly 770 g/mol in ~48 hrs at 40 °C. Given the rate of biological growth and conversion this rate of throughout in the depolymerization step may not be prohibitive. Finally, CMF depolymerization of LS need not be considered in isolation, but rather could be employed subsequent to a process that releases aromatic monomers. The fact that depolymerization occurs in aqueous solutions at mild conditions should allow the depolymerization and fermentation processes to be coupled, lowering processing costs.

5. CONCLUSIONS

Depolymerization of lignin followed by biological conversion of the breakdown products has the potential to supply valuable compounds that are currently derived from petroleum. However, for natural lignins isolated from carbohydrate-first pretreatment processes cleaving C-C bonds will be essential to recover a high fraction of the mass as low molecular weight products. Current approaches face challenges due to high cost, difficulty in avoiding repolymerization, toxicity of some of the products, and low bioconversion. Here we introduce an alternative approach, demonstrating that a chelator-mediated Fenton reaction efficiently cleaves C-C bonds in lignosulfonate at or near room temperature. We also show that repolymerization can be minimized through careful control of reagent concentrations and reaction temperature. Initial studies of growth of monocultures on the lignosulfonate depolymerization products show promise, especially when supplemented with a small amount of glucose.

AUTHOR'S CONTRIBUTIONS

M. S. K. conceived and designed the experiments and supervised the project. D. V. M. and M. A. J. performed the Fenton reactions and SEC analysis. A. R. performed the growth experiments and the melanin content assay. E. J. M. performed the FTIR measurements. T. M. A. performed the NMR measurements. B. A. S., K. L. S., and S. W. S. consulted on the project. All authors read and approved the final manuscript.

AUTHOR'S INFORMATION

Corresponding Author

Michael S. Kent
Sandia National Labs and the Joint BioEnergy Institute

mskent@sandia.gov

Conflict of Interest

There are no conflicts of interest to declare.

Acknowledgments

This work was part of the DOE Joint BioEnergy Institute (http://www.jbei.org) supported by the U.S. Department of Energy, Office of Science, Office of Biological and Environmental Research, through contract DE-AC02-05CH11231 between Lawrence Berkeley National Laboratory and the U.S. Department of Energy. Sandia National Laboratories is a multi-mission laboratory managed and operated by National Technology and Engineering Solutions of Sandia, LLC., a wholly owned subsidiary of Honeywell International, Inc., for the U.S. Department of Energy's National Nuclear Security Administration under contract DE-NA-0003525. Note: This paper describes objective technical results and analyses. Any subjective views or opinions that might be expressed in the paper do not necessarily represent the views of the U.S. Department of Energy or the United States Government.

Notes and References

[1] R. Davis, N. Grundl, L. Tao, M.J. Biddy, E.C.D. Tan, G.T. Beckham, D. Humbird, D.N. Thompson, M.S. Roni, Process design and economics for the conversion of lignocellulosic biomass to hydrocarbon fuels and coproducts: 2018 biochemical design case update, National Renewable Energy Laboratory, 2018.
[2] L. Cao, I.K.M. Yu, Y. Liu, X. Ruan, D.C.W. Tsang, A.J. Hunt, Y.S. Ok, H. Song, S. Zhang, lignin valorization for the production of renewable chemicals: State-of-the-art review and future prospects, Bioresource Technology 269 (2018) 465-475.
[3] R.-C. Sun, J.S.M. Samec, A.J. Ragauskas, Preface to special Issue of ChemSusChem on Lignin Valorization: From theory to practice, ChemSusChem 13 (2020) 4175-4180.
[4] Z. Chen, C. Wan, Biological valorization stratgies for converting lignin into fuels and chemicals, Renewable and Sustainable Energy Reviews 73 (2017) 610-621.

[5] G.T. Beckham, C.W. Johnson, E.M. Karp, D. Salvachúa, D.R. Vardon, Opportunities and challenges in biological lignin valorization, Current Opinion in Biotechnology 42 (2016) 40-53.
[6] O.Y. Abdelaziz, D.P. Brink, J. Prothmann, K. Ravi, M. Sun, J. García-Hidalgo, M. Sandahl, C.P. Hulteberg, C. Turner, G. Lidén, M.F. Gorwa-Grauslund, Biological valorization of low molecular weight lignin, Biotechnology Advances 34 (2016) 1318-1346.
[7] M. Kumar, S. You, J. Beiyuan, G. Luo, J. Gupta, S. Kumar, L. Singh, S. Zhang, D.C.W. Tsang, Lignin valorization by bacterial genus *Pseudomonas*: State-of-the-art review and prospects, Bioresourse Technology 320 (2021) 124412.
[8] J.G. Linger, D.R. Vardon, M.T. Guarnieri, E.M. Karp, G.B. Hunsinger, M.A. Franden, C.W. Johnson, G. Chupka, T.J. Strathmann, P.T. Pienkos, G.T. Beckham, Lignin valorization through integrated biological funneling and chemical catalysis, Proc. Nat. Acad. Sci. 111 (2014) 12013-12018.
[9] A. Rodriguez, D. Salvachúa, R. Katahira, B.A. Black, N.S. Cleveland, M. Reed, H. Smith, E.E.K. Baidoo, J.D. Keasling, B.A. Simmons, G.T. Beckham, J.M. Gladden, Base-catalyzed depolymerization of solid lignin-rich streams enables microbial conversion, ACS Sustainable Chemistry & Engineering 5 (2017) 8171-8180.
[10] C.S. Lancefield, O.S. Ojo, F. Tran, N.J. Westwood, Isolation of functionalized phenolic monomers through selective oxidation and C-O bond cleavage of the β-O-4 linkages in lignin, Angewandt Communications 54 (2015) 258-262.
[11] L. Shuai, M.T. Amiri, Y.M. Questell-Sandiago, F. Héroguel, Y. Li, H. Kim, R. Meilan, C. Chapple, J. Ralph, J.S. Luterbacher, Formaldehyde stabilization facilitates lignin monomer production during biomass depolymerization, Science 354 (2016) 329-333.
[12] P. Picart, H. Liu, G.P. M., N. Anders, L. Zhu, J. Klankermayer, W. Leitner, P. Domínguez de María, U. Schwaneberg, A. Schallmey, Multi-step biocatalytic depolymerization of lignin, Appl Microbiol Biotechnol 101 (2017) 6277-6287.
[13] A. Rahimi, A. Ulbrich, J.J. Coon, S.S. Stahl, Formic-acid-induced depolymerization of oxidized lignin to aromatics, Nature 515 (2014) 249-252.
[14] W.J. Sagues, H. Bao, J.L. Nemenyi, Z. Tong, Lignin-first approach to biorefining: utilizing Fenton's reagent and supercritical ethanol for the production of phenolics an sugars, ACS Sustainable Chem. Eng. 6 (2018) 4958-4965.
[15] R. Katahira, A. Mittal, M. Kellene, X. Chen, M.P. Tucker, D.K. Johnson, G.T. Beckham, Base-catalyzed depolymerization of biorefinery lignins, ACS Sustainable Chem. Eng. 4(3) (2016) 1474-1486.
[16] G.E. Klinger, Y. Zhou, J.A. Foote, A.M. Wester, Y. Cui, M. Alherech, S.S. Stahl, J.E. Jackson, E.L. Hegg, Nucleophilic thiols reductively cleave ether linkages in lignin model polymers and lignin ChemSusChem 13 (2020) 1-7.
[17] T. Phongpreecha, N.C. Hool, R.J. Stoklosa, A.S. Klett, C.E. Foster, A. Bhalla, D. Holmes, M.C. Thies, D.B. Hodge, Predicting lignin depolymerization yields from quantifiable properties using fractionated biorefinery lignins, Green Chemistry 19 (2017) 5131-5143.
[18] S. Wang, W.-X. Li, Y.-Q. Yang, X. Chen, J. Ma, C. Chen, X. L.-P., R.-C. Sun, Unlocking structure-reactivity relationships for catalytic hydrogenolysis of lignin into phenolic monomers, ChemSusChem 13 (2020) 4548-4556.
[19] Q. Song, F. Wang, J. Cai, Y. Wang, J. Zhang, W. Yu, J. Xu, Lignin depolymerization (LDP) in alcohol over nickel-based catalysts via a fragmentation-hydrogenolysis process, Energy & Environmental Science 6 (2013) 994-1007.
[20] S. Van den Bosch, W. Schutyser, R. Vanholme, T. Driessen, S.-F. Koelewijn, T. Renders, B. De Meester, W.J.J. Huijgen, W. Dehaen, C.M. Courtin, B. Lagrain, W. Boerjan, B.F. Sels, Reductive lignocellulose frationation into soluble lignin-derived phenolic monomers and dimers and processable carbohydrate pulps, Energy and Environmental Science 8 (2015) 1748-1763.
[21] E.M. Anderson, R. Katahira, M. Reed, M.G. Resch, E.M. Karp, G.T. Beckham, Y. Román-Leshkov, Reductive catalytic fractionation of corn stover lignin, ACS Sustainable Chem. Eng. 4 (2016) 6940-6950.
[22] H. Luo, I.M. Klein, Y. Jiang, J. Zhu, B. Liu, H.I. Kenttamaa, M.M. Abu-Omar, Total utilization of miscanthus biomass, lignin and carbohydrates, using earth abundant nickel catalyst, ACS Sustainable Chem. Eng. 4 (2016) 2316-2322.
[23] J. Zakzeski, P.C.A. Bruijnincx, A.L. Jongerius, B.M. Weckhuysen, The catalytic valorization of lignin for the production of renewable chemicals, Chemical Reviews 110 (2010) 3552-3599.
[24] H. Wang, M. Tucker, Y. Ji, Recent development in chemical depolymerization of lignin: A review, Journal of Applied Chemistry 2013 (2013) 1-9.
[25] A.K. Deepa, P.L. Dhepe, Lignin depolymerization into aromatic monomers over solid acid catalysts, ACS Catalysis 5 (2014) 365-379.
[26] W. Lan, M.T. Amiri, C.M. Hunston, J.S. Luterbacher, Protection group effects during a, g-diol lignin stabilization promote high-selectivity monomer production Angewandte Chemie Int. Ed. 57 (2018) 1356-1360.
[27] M. Tschulkow, T. Compernolle, S. Van den Bosch, J. Van Aelst, I. Storms, M. Van Dael, G. Van den Bossche, B. Sels, S. Van Passel, Integrated techno-economic assessment of a biorefinery process: The high-end valorization of the lignocellulosic fraction in wood streams, Journal of Cleaner Production 266 (2020) 122022.
[28] T. Korányi, B. Fridrich, A. Pineda, K. Barta, Development of 'lignin-first' approaches for the valorization of lignocellulosic biomass, Molecules 25 (2020) 2815.
[29] D. Salvachúa, R. Katahira, N.S. Cleveland, P. Khanna, M.G. Resch, B.A. Black, S.O. Purvine, E.M. Zink, A. Prieto, M.J. Martínez, B.A. Simmons, J.M. Gladden, G.T. Beckham, Lignin depolymerization by fungal secretomes and a microbial sink, Green Chemistry 18 (2016) 6046-6062.
[30] C.A. Gasser, M. Čvančarová, E.M. Ammann, A. Schäffer, P. Shahgaldian, P.F.-X. Corvini, Sequential lignin depolymerization by combination of biocatalytic and formic acid/formate treatment steps Appl Microbiol Biotechnol 101 (2017) 2575-2588.
[31] H. Lange, S. Decina, C. Crestini, Oxidative upgrade of lignin - Recent routes reviewed, European Polymer Journal 49 (2013) 1151-1173.
[32] K.E. Hammel, D. Cullen, Role of fungal peroxidases in biological ligninolysis, Current Opinion in Plant Biology 11 (2008) 349-355.
[33] J.C. Chan, M. Paice, X. Zhang, Enzymatic oxidation of lignin: Challenges and barriers toward practical applications, ChemCatChem 12 (2020) 401-425.
[34] L.M.C. Leynaud Kieffer Curran, L.T.M. Pham, K.L. Sale, B.A. Simmons, Review of advances in the development of laccases for the valorization of lignin to enable production of lignocellulosic biofuels and bioproducts, Biotechnology Advances in press (2021) 107809.
[35] C.-F. Chow, W.-L. Wong, K.Y.-F. Ho, C.-S. Chan, C.-B. Gong, Combined chemical activation and fenton degradation to convert waste polyethylene into high-value fine chemicals Chem. Eur. J. 22 (2016) 9513-9518.
[36] H.-M. Feng, J.-C. Zheng, N.-Y. Lei, L. Yu, K.H.-K. Kong, H.-Q. Yu, T.-C. Lau, M.H.W. Lam, Photoassisted fenton degradation of polystyrene Environ. Sci. Technol. 45 (2011) 744-750.

[37] M.C. Krueger, U. Hofmann, M. Moeder, D. Schlosser, Potential of wood-rotting fungi to attack polystyrene sulfonate and its depolymerisation by gloeophyllum trabeum via hydroquinone-driven fenton chemistry PLoS ONE 10 (2015) e0131773.
[38] D. Areskogh, G. Henriksson, Fenton's reaction: a simple and versatile method to structurally modify commercial lignosulphonates, Nordic Pulp and Paper Research Journal 26 (2011) 90-98.
[39] B. Fernandes, T. Matamá, D. Guimarães, A. Gomes, A. Cavaco-Paulo, Fluorescent quantification of melanin, Pigment Cell & Melanoma Research 29 (2016) 707-712.
[40] H.D. Magurudeniya, N.R. Baral, A. Rodriquez, C.D. Scown, J. Dahlberg, D. Putnam, A. George, B. SImmons, A., J.M. Gladden, Use of ensiled biomass sorghum increases ionic liquid pretreatment efficiency and reduces biofuel production cost and carbon footprint, Green Chem. 23 (2021) 3127-3140.
[41] H. Sixta, A. Potthast, A.W. Krotschek, Chemical pulping processes, in: H. Sixta (Ed.), Handbook of Pulp, WILEY-VCH Verlag GmbH & Co., Weinheim, , 2006, pp. 109-509.
[42] J.C. Yang, M.J. Jablonsky, J.W. Mays, NMR and FT-IR studies of sulfonated styrene-based homopolymers and copolymers, Polymer 43 (2002) 5125-5132.
[43] R. De, H. Lee, B. Das, Exploring the interactions in binary mixtures of polyelectrolytes: Influense of mixture composition, concentration, and temperature on counterion condensation, Journal of Molecular Liquids 251 (2018) 94-99.
[44] G. Zundel, Chapter II Assignment of the IR bands, Hydration and intermolecular interaction: Infrared investigations with polyelectrolyte membranes, Elsevier Science and Technology1970.
[45] J.-J. Max, C. Chapados, Infrared spectroscopy of aqueous carboxylic acids: malic acid, J. Phys. Chem. A 106 (2002) 6452-6461.
[46] A.V. Kalliola, T.; Liitiä, T.; Tamminen, T., Alkali-O2 oxidized lignin-a bio-based concrete plasticizer, Industrial Crops and Products 74 (2015) 150-157.
[47] P. Rodriguéz-Lucena, J.J. Lucena, L. Hernández-Apaolaza, Relationship between the structure of Fe-lignosulfonate coplexes determined by FTIR spectroscopy and their reduction by the leaf Fe reductase, International Plant Nutrition Colloquium XVI, UC Davis: Department of Plant Sciences, 2009.
[48] C. Boeriu, D. Bravo, R.J.A. Gosselink, J.E.G. van Dam, Characterization of structure-dependent functional properties of lignin with infrared spectroscopy, Industrial Crops and Products 20 (2004) 205-218.
[49] F. Asgari, D.S. Argyropoulos, Fundamentals of oxygen delignification. Part II. Functional group formation/elimination in residual kraft lignin, Can. J. Chem. 76 (1998) 1606-1615.
[50] J. Zeng, C.G. Yoo, F. Wang, X. Pan, W. Vermerris, Z. Tong, Biomimetic Fenton-catalysed lignin depolymerization to high-value aromatics and dicarboxylic acids, ChemSusChem 8 (2015) 861-871.
[51] L. Hildén, G. Johansson, G. Pettersson, J. Li, P. Ljungquist, G. Henricksson, Do the extracellular enzymes cellobiose dehydrogenase and manganese peroxidase form a pathwy in lignin biodegradation?, FEBS Lett. 477 (2000) 79-83.
[52] A.P. Marques, D.V. Evtuguin, S. Magina, F.M.L. AMado, A. Prates, Structure of lignosulfonates from acidic magnesium-based sulphite pulping of *Eucalyyptus globulus*, Journal of Wood Chemistry and Technology 29 (2009) 337-357.
[53] D.V. Evtuguin, G. Rocha, B.J. Goodfellow, Detection of muconic acid type strucrues in oxidised lignins using 2D NMR spectroscpy, Holzforschung 63 (2009) 675-680.
[54] W.L. Schroeder, S.D. Harris, R. Saha, Computation-driven analysis of model polyextremo-tolerant fungus *Exophiala dermatitidis*: Defensive pigment metabolic costs and human applications, iScience 23 (2020) 100980.
[55] M. Cheriyan, E.J. Toone, C.A. Fierke, Improving upon nature: active site remodeling produces highly efficient aldolase activity toward hdrophobic electrophilic substrates, Biochemistry 51 (2012) 1658-1668.
[56] G. G., b-diketone hydrolases, Journal of Molecular Catalysis B: Enzymatic 19-20 (2002) 73-82.
[57] M. Leisola, B.H. Schmidt, U. Thanei-Wyss, A. Fiechter, Aromatic ring cleavage of veratryl alcohol by *Phanerochaete chrysosporium*, FEBS Letters 189 (1985) 267-270.
[58] T. Umezawa, T. Higuchi, Mechanism of aromatic ring cleavage of b-O-4 lignin substructure models by lignin peroxidase, FEBS Letters 218 (1987) 255-260.
[59] L.T.M. Pham, K. Deng, T.R. Northern, S.W. Singer, P.D. Adams, B.A. Simmons, K.L. Sale, Experimental and theoretical insights into the effects of pH on catalysis of bond-cleavage by the lignin peroxidase isozyme H8 from Phanerochaete chrysosporium, Biotechnology for Biofuels 14 (2021) 108.
[60] J. Dillies, C. Vivien, M. Chevalier, A. Rulence, G. Châtaigne, C. Flahaut, V. Senez, R. Froidevaux, Enzymatic depolymerization of industrial lignins by laccase-mediator systems in 1,4-dioxane/water, Biotechnology and Applied Biochemistry 67 (2020) 774-782.
[61] M.S. Kent, J. Zeng, N. Rader, I.C. Avina, C.T. Simoes, C.K. Brenden, M.L. Busse, J.D. Watt, N.H. Giron, T.M. Alam, M.D. Allendorf, B.A. Simmons, N.S. Bell, K.L. Sale, Efficient conversion of lignin into a water-soluble polymer by a chelator-mediated Fenton reaction: optimization of H2O2 use and performance as a dispersant, Green Chemistry 20 (2018) 3024-3037.
[62] W.A. Pryor, Oxy-radicals and related species, Ann. Rev. Physiol. 48 (1986) 657-667.
[63] A. Barapatre, A.S. Meena, S. Mekala, A. Das, H. Jha, *In vitro* evaluation of antioxidant and cytotoxic activities of lignin fractions extracted from *Acacia nilotica*, international Journal of Biological Macromolecules 86 (2016) 443-453.
[64] P. Salgado, V. Melin, Y. Durán, H. Mansilla, D. Contreras, The reactivity and reaction pathway of Fenton reactions driven by substituted 1,2-dihydroxybenzenes, Environmental Science & Technology 51 (2017) 3687-3693.
[65] D.R. Contreras, J.; Freer, J.; Schwederski, B.; Kaim, W., Enhanced hydroxyl radical production by dihydroxybenzene-driven Fenton reactions: implications for wood biodegradation, J Biol Inorg Chem 12 (2007) 1055-1061.
[66] V.M. Arantes, A.M.F., The effect of a catecholate chelator as a redox agent in Fenton-based reactions on degredation of lignin-model substrates and on COD removal from effluent of an ECF kraft pulp mill, Journal of Hazardous Materials 141 (2007) 273-279.
[67] A. Aguiar, A. Ferraz, Fe^{3+} and Cu^{2+} -reduction by phenol derivatives associated with Azure B degradation in Fenton-like reactions, Chemosphere 66 (2007) 947-954.
[68] V. Arantes, J. Jellison, B. Goodell, Peculiarities of brown-rot fungi and biochemical Fenton reaction with regard to their potential s a model for bioprocessng biomass, Appl Microbiol Biotechnol 94 (2012) 323-338.
[69] V. Arantes, A.M.F. Milagres, T.R. Filley, B. Goodell, Lignocellulosic polysaccharides and lignin degradation by wood decay fungi: the relevance of nonenzymatic Fenton-based reactions, J Ind Microbiol Biotechnol 38 (2011) 541-555.
[70] V. Melin, A. Henríquez, C. Radojkovic, B. Schwederski, W. Kaim, J. Freer, D. Contreras, Reduction reactivity of catecholamines and their ability to promote a Fenton reaction, Inorganic Chimica Acta 453 (2016) 1-7.

[71] V.B. Arantes, C.; Milagres, A.M.F., Degradation and decolorization of a biodegradable-resistant polymeric dye by chelator-mediated Fenton reactions, Chemosphere 63 (2006) 1764-1772.
[72] W.A. Pieken, J.W. Kozarich, lactonization of cis, cis-3-halomuconates: influence of pH and halo substituent on the regiochemistry, J. Org. Chem. 55 (1990) 3029-3035.